Universiteit Leiden
The Netherlands

A binding kinetics study of human adenosine A(3) receptor agonists

Xia, L.Z.; Kyrizaki, A.; Tosh, D.K.; Duijl, T.T. van; Roorda, J.C.; Jacobson, K.A.; ... ; Heitman, L.H.

A binding kinetics study of human adenosine A₃ receptor agonists

Lizi Xia [a], Athina Kyrizaki [a], Dilip K. Tosh [b], Tirsa T. van Duijl [a], Jacomina Cornelia Roorda [a], Kenneth A. Jacobson [b], Adriaan P. IJzerman [a], Laura H. Heitman [a,*]

[a] Division of Medicinal Chemistry, LACDR, Leiden University, The Netherlands
[b] Laboratory of Bioorganic Chemistry, National Institute of Diabetes & Digestive & Kidney Diseases, National Institutes of Health, Bethesda, MD, USA

ARTICLE INFO

ABSTRACT

The human adenosine A₃ (hA₃) receptor has been suggested as a viable drug target in inflammatory diseases and in cancer. So far, a number of selective hA₃ receptor agonists (e.g. IB-MECA and 2-Cl-IB-MECA) inducing anti-inflammatory or anticancer effects are under clinical investigation. Drug-target binding kinetics is increasingly recognized as another pharmacological parameter, next to affinity, for compound triage in the early phases of drug discovery. However, such a kinetics-driven analysis has not yet been performed for the hA₃ receptor. In this study, we first validated a competition association assay for adenosine A₃ receptor agonists to determine the target interaction kinetics. Affinities and Kinetic Rate Index (KRI) values of 11 ribofurano and 10 methanocarba nucleosides were determined in radioligand binding assays. Afterwards, 15 analogues were further selected (KRI <0.70 or KRI >1.35) for full kinetics characterization. The structure-kinetics relationships (SKR) were derived and longer residence times were associated with methanocarba and enlarged adenine N^6 and C2 substitutions. In addition, from a k_{on}-k_{off}-K_D kinetic map we divided the agonists into three subgroups. A residence time "cliff" was observed, which might be relevant to (N)-methanocarba derivatives' rigid C2-arylalkynyl substitutions. Our findings provide substantial evidence that, next to affinity, additional knowledge of binding kinetics is useful for developing and selecting new hA₃R agonists in the early phase of the drug discovery process.

1. Introduction

The adenosine A₃ receptor is the youngest member discovered in the family of adenosine receptors (A₁, A₂ₐ, A₂ᵦ and A₃), all of which belong to class A G protein-coupled receptors (GPCR) [1]. Unlike the other subtypes, the adenosine A₃ receptor is endogenously activated by both adenosine and inosine [2]. Following agonist activation, the receptor causes a decrease in cAMP levels as it primarily couples to Gᵢ protein. The adenosine A₃ receptor is widely distributed throughout the body, albeit at low expression levels, and its activation can affect numerous organs, tissues and systems. However, this receptor is overexpressed in inflammatory and cancer cells, reflecting its importance as a therapeutic target and biological marker in these tissues [3,4]. Moreover, the adenosine A₃ receptor is rapidly internalized within 30 min after agonist exposure [5,6]. It is unresolved whether receptor desensitization terminates agonist-induced signaling or if this signaling persists after internalization [7].

Since agonists cause effects of anti-inflammation, cardioprotection and neuroprotection, numerous potent and selective agonists have been extensively studied and developed [8–13]. Most of these agonists are derivatives of adenosine, with substitutions on the adenine nucleobase or the ribose moiety. In particular, IB-MECA and 2-Cl-IB-MECA are two potent clinical candidates with excellent bioavailability and safety profiles. Selective hA₃ receptor agonists are being evaluated for the treatment of chronic inflammatory diseases (e.g., rheumatoid arthritis or psoriasis), neuropathic pain and cancer (i.e. hepatocellular carcinoma) [14–17].

Traditional drug discovery approaches mainly focus on affinity, a parameter that is defined under equilibrium conditions. However, it is emerging that selecting ligands based on their affinity alone, does not necessarily predict *in vivo* efficacy very well. This may be due to the dynamic conditions *in vivo*, that often are in contrast to the equilibrium conditions applied in *in vitro* assays [18]. In fact a ligand's kinetic properties may provide a better indication of how a ligand will perform *in vivo* [19]. Notably, the parameter of residence time (RT) has been proposed as a more relevant selection criterion. The RT reflects the lifetime of the ligand-receptor complex and can be calculated as the reciprocal of the ligand's dissociation constant [20,21].

Although the binding kinetics of hA$_3$ receptor agonists are occasionally reported [22,23], a systematic kinetics analysis yielding structure-kinetics relationships (SKR) has not been conducted. Therefore, we firstly validated the binding kinetics of the prototypical hA$_3$ receptor agonists (i.e. IB-MECA and 2-Cl-IB-MECA), using radioligand displacement and competition association assays. Then, two series of ribofurano and methanocarba ([3.1.0]bicyclohexane) adenosine derivatives were evaluated for both their affinity (K$_i$) and kinetics (Kinetic Rate Index (KRI) values, k$_{on}$, k$_{off}$, and RTs). This allowed a complete SKR analysis next to a more traditional SAR study. Afterwards, a retrospective evaluation linking residence times and *in vivo* efficacies was discussed. Last but not least, from a k$_{on}$-k$_{off}$-K$_D$ kinetic map we divided the agonists into three subgroups, providing a possible direction for the further development of hA$_3$R agonists.

2. Materials & Methods

2.1. Chemicals and reagents

[^{3}H]8-Ethyl-4-methyl-2-phenyl-(8*R*)-4,5,7,8-tetrahydro-1*H*-imidazo[2,1-*i*]-purin-5-one ([^{3}H]PSB-11, specific activity 56 Ci·mmol^{-1}) was obtained with the kind help of Prof. C.E. Müller (University of Bonn, Germany). 5′-*N*-methylcarboxamidoadenosine (MECA) was provided by one of the authors (KAJ). Unlabeled PSB-11, 1-deoxy-1-[6-[((3-Iodophenyl)methyl)amino]-9H-purin-9-yl]-N-methyl-β-ᴅ-ribofuranuronamide (IB-MECA), and 2-chloro-*N*^{6}-(3-iodobenzyl)-adenosine-5′-N-methyluronamide (2-Cl-IB-MECA) were purchased from Tocris Ltd. (Abingdon, UK). 5′-*N*-ethylcarboxamidoadenosine (NECA) was purchased from Sigma-Aldrich (Steinheim, Germany). LUF5501, LUF5505, LUF5500, LUF5506 and LUF5521 have been synthesized and described previously by de Zwart et al. [24]; LUF5595, LUF5586 and LUF5589 have been described by van Tilburg et al. [25]; MRS7140, MRS5980, MRS7154, MRS7549, MRS5655, MRS5679, MRS5698, MRS5644, MRS5667 and MRS7294 have been described by Tosh et al. [26–29], and MRS3558 by Tchilibon et al. [30]. Adenosine deaminase (ADA) was purchased from Boehringer Mannheim (Mannheim, Germany). Bicinchoninic acid (BCA) and BCA protein assay reagents were purchased from Pierce Chemical Company (Rockford, IL, USA). Chinese hamster ovary (CHO) cells stably expressing the human adenosine A$_3$ receptor (CHOhA$_3$) were a gift from Dr. K-N Klotz (University of Würzburg, Germany). All other chemicals were obtained from standard commercial sources and were of analytical grade.

2.2. Cell culture and membrane preparation

CHOhA$_3$ cells were cultured and membranes were prepared and stored as previously described [22]. Protein determination was done through the use of the bicinchoninic acid (BCA) method [31].

2.3. Radioligand equilibrium displacement assays

Membrane aliquots containing ~15 µg of CHOhA$_3$ protein were incubated in a total volume of 100 µL assay buffer (50 mM Tris-HCl, 5 mM MgCl$_2$, supplemented with 0.01% CHAPS and 1 mM EDTA, pH 7.4) at 10 °C for 240 min. Displacement experiments were performed using 6 concentrations of competing agonist in the presence of a final concentration of ~10 nM [^{3}H]PSB-11. At this concentration, total radioligand binding did not exceed 10% of that added to prevent ligand depletion. Nonspecific binding (NSB) was determined in the presence of 100 µM NECA. Incubation was terminated by rapid filtration performed on 96-well GF/B filter plates (Perkin Elmer, Groningen, the Netherlands), using a PerkinElmer Filtermate-harvester (Perkin Elmer, Gronin-

gen, the Netherlands). After drying the filter plate at 50 °C for 30 min, the filter-bound radioactivity was determined by scintillation spectrometry using the 2450 MicroBeta^2 Plate Counter (Perkin Elmer, Boston, MA).

2.4. Radioligand competition association assays

The binding kinetics of unlabeled ligands were quantified using the competition association assay based on the theoretical framework by Motulsky and Mahan [32]. The competition association assay was initiated by adding membrane aliquots (15 µg/well) at different time points for a total of 240 min to a total volume of 100 µL of assay buffer at 10 °C with ~10 nM [^{3}H]PSB-11 in the absence or presence of a single concentration of competing hA$_3$ receptor agonists (i.e. at their IC$_{50}$ value), and, in some experiments indicated, in the simultaneous presence of 1 mM GTP. Incubations were terminated and samples were obtained as described under *Radioligand Displacement Assay*. The "dual-point" competition association assays were designed as described previously [33], where in this case the two time points were selected at 20 min (t$_1$) and 240 min (t$_2$).

2.5. Data analysis

All experimental data were analyzed using the nonlinear regression curve fitting program GraphPad Prism 7.0 (GraphPad Software, Inc., San Diego, CA). From displacement assays, IC$_{50}$ values were obtained by non-linear regression analysis of the displacement curves. The obtained IC$_{50}$ values were converted into K$_i$ values using the Cheng-Prusoff equation to determine the affinity of the ligands [34], using a K$_D$ value for the radioligand of 1.04 nM at 10 °C as determined from radioligand association and dissociation assays, as previously reported [35]. The residence time (RT, in min) was calculated using the equation RT = 1/(60 * k$_{off}$), as k$_{off}$ is in s^{-1}. Association and dissociation rate constants for unlabeled compounds were calculated by fitting the data into the competition association model using "kinetics of competitive binding":

$$K_A = k_1[L] \cdot 10^{-9} + k_2$$
$$K_B = k_3[I] \cdot 10^{-9} + k_4$$
$$S = \sqrt{(K_A - K_B)^2 + 4 \cdot k_1 \cdot k_3 \cdot L \cdot I \cdot 10^{-18}}$$
$$K_F = 0.5(K_A + K_B + S)$$
$$K_S = 0.5(K_A + K_B - S)$$
$$Q = \frac{B_{max} \cdot k_1 \cdot L \cdot 10^{-9}}{K_F - K_S}$$
$$Y = Q \cdot \left(\frac{k_4 \cdot (K_F - K_S)}{K_F \cdot K_S} + \frac{k_4 - K_F}{K_F} e^{(-K_F \cdot X)} - \frac{k_4 - K_S}{K_S} e^{(-K_S \cdot X)} \right)$$

where k$_1$ is the k$_{on}$ of the radioligand (M^{-1} s^{-1}), k$_2$ is the k$_{off}$ of the radioligand (s^{-1}), L is the radioligand concentration (nM), I is the concentration of the unlabeled competitor (nM), X is the time (s) and Y is the specific binding of the radioligand (DPM). The control curve (without competitor) from competition association assays generates the k$_1$ value, and the k$_2$ value was obtained from previous radioligand association and dissociation assays [35]. With that the k$_3$, k$_4$ and B$_{max}$ were calculated, where k$_3$ represents the k$_{on}$ (M^{-1} s^{-1}) of the unlabeled ligand, k$_4$ stands for the k$_{off}$ (s^{-1}) of the unlabeled ligand and B$_{max}$ equals the total binding (DPM). All competition association data were globally fitted.

3. Results

3.1. The effects of GTP on affinities and kinetics of the reference hA$_3$ receptor agonists IB-MECA and 2-Cl-IB-MECA

Firstly, we determined the effects of GTP (1 mM) on both the affinities and binding kinetics of the reference hA$_3$ receptor ago-

Table 1
The effects of GTP (1 mM) on the affinities and kinetics of hA$_3$ receptor agonists IB-MECA and 2-Cl-IB-MECA.

Agonists	pK$_i$ (mean K$_i$ in nM)[a]	Hill Slope [a]	KRI[b]	k$_{on}$ (M^{-1} s^{-1})[c]	k$_{off}$ (s^{-1})[d]	RT (min)[e]	Kinetic K$_D$ (mean pK$_D$)[f]
no GTP							
IB-MECA	8.5 ± 0.07*** (2.9)	−0.94 ± 0.05 ns	1.55 ± 0.07**	(5.9 ± 0.9) × 10^5 ns	(1.8 ± 0.2) × 10^{-4} ns	95 ± 13*	0.30 ± 0.06 (9.5)
2-Cl-IB-MECA	8.5 ± 0.1* (3.5)	−0.85 ± 0.21 ns	2.02 ± 0.06***	(4.0 ± 0.5) × 10^5 ns	(7.2 ± 1.1) × 10^{-5}*	231 ± 34*	0.18 ± 0.04 (9.7)
+ 1 mM GTP							
IB-MECA	8.0 ± 0.02 (11)	−0.99 ± 0.07	0.99 ± 0.08	(4.5 ± 2.5) × 10^5	(8.5 ± 3.0) x 10^{-4}	20 ± 7	1.9 ± 1.2 (8.7)
2-Cl-IB-MECA	8.0 ± 0.08 (10)	−1.1 ± 0.1	1.07 ± 0.07	(4.0 ± 2.3) × 10^5	(5.7 ± 1.5) × 10^{-4}	29 ± 8	1.4 ± 0.9 (8.9)

Student's *t*-test was applied for the comparison of values of pK$_i$, KRI, k$_{on}$, k$_{off}$, RT obtained in the absence vs presence of GTP (1 mM) in the assay conditions, ***p < .0005, **p < .005, *p < .05, ns for not significant.

[a] pK$_i$ ± SEM (n ≥ 3, mean K$_i$ value in nM), obtained from radioligand binding assays with [3H]PSB-11 on the hA$_3$ receptor stably expressed on CHO cell membranes.
[b] KRI ± SEM (n = 3) obtained from dual-point competition association assays with [3H]PSB-11 on the hA$_3$ receptor stably expressed on CHO cell membranes.
[c] k$_{on}$ ± SEM (n ≥ 3), obtained from competition association assays with [3H]PSB-11 on the hA$_3$ receptor stably expressed on CHO cell membranes.
[d] k$_{off}$ ± SEM (n ≥ 3), obtained from competition association assays with [3H]PSB-11 on the hA$_3$ receptor stably expressed on CHO cell membranes.
[e] RT = 1/(60 * k$_{off}$); RT is expressed in min, whereas k$_{off}$ is expressed in s^{-1}.
[f] K$_D$ = k$_{off}$/k$_{on}$.

nists IB-MECA and 2-Cl-IB-MECA. Under the two different assay conditions (i.e. in the absence or presence of GTP) the affinities of IB-MECA and 2-Cl-IB-MECA were significantly different (Table 1). We observed a rightward shift of the displacement curves in the presence of GTP (Fig. 1A, closed symbols), representing an approx. 3-Fold decrease in affinity for both compounds. Of note, under both experimental conditions, monophasic displacement curves were obtained with pseudo-Hill coefficients close to unity (Table 1).

Furthermore, there were significant differences between the kinetics of hA$_3$ receptor agonists tested in the absence or presence of 1 mM GTP. In the competition association assays without GTP, both IB-MECA and 2-Cl-IB-MECA produced a typical "overshoot", representative of a slower dissociation from the hA$_3$ receptor than the radioligand [3H]PSB-11 (Fig. 1B). This overshoot, however, disappeared in the experiments with GTP (Fig. 1C). Thus, their KRI values were decreased from well-above-unity in the absence of GTP to close-to-unity in the presence of GTP. The k$_{off}$ values of IB-MECA and 2-Cl-IB-MECA determined by the Motulsky-Mahan model [32] were (1.8 ± 0.2) × 10^{-4} s^{-1} and (7.2 ± 1.1) × 10^{-5} s^{-1} in the absence of GTP, respectively (Table 1), which were smaller than the corresponding values determined in the presence of GTP (IB-MECA: (8.5 ± 3.0) × 10^{-4} s^{-1}; 2-Cl-IB-MECA: (5.7 ± 1.5) × 10^{-4} s^{-1}, Table 1). Consequently, the calculated RTs in the absence of GTP were longer than the values derived when GTP was present (IB-MECA: 95 min vs 20 min; 2-Cl-IB-MECA 231 min vs 29 min, Table 1). Last but not least, the k$_{on}$ values of these two agonists determined under the two assay conditions were similar. Therefore, in order to define a more agonist-relevant receptor interaction, we decided to use the competition association assay in the absence of GTP for the determination of the affinities and the binding kinetics of other unlabeled hA$_3$ receptor agonists in the remainder of the study.

3.2. Binding affinity (K$_i$) of hA$_3$ receptor agonists

The binding affinities of 22 human A$_3$ receptor agonists in total were determined in equilibrium radioligand displacement studies. All agonists were able to concentration-dependently inhibit specific [3H]PSB-11 binding to the human A$_3$ receptor and their affinities are listed in Tables 2 and 3. The agonists displayed moderate to high binding affinities, ranging from 82 nM for agonist MRS5679 to 0.72 nM for agonist MRS5980, while the reference agonists IB-MECA and 2-Cl-IB-MECA had an affinity of 2.9 and 3.5 nM, respectively.

3.3. KRI values of hA$_3$ receptor agonists

Subsequently, these hA$_3$ receptor agonists were screened in what is termed a "dual-point" competition association assay. The

specific binding of [3H]PSB-11 was measured after 20 and 240 min in the absence and presence of a single concentration (i.e. IC$_{50}$) of unlabeled hA$_3$ receptor agonists, which yielded their KRI values. The KRI values of the hA$_3$ receptor agonists ranged from 0.64 (LUF5501) to 5.56 (MRS5679) (Tables 2 and 3). Agonists with a KRI value larger than unity are considered to have a slower dissociation rate, and thus a longer RT, than the radioligand used, i.e. [3H]PSB-11, and *vice versa*. Agonists having KRI values below 0.70 (LUF5501 and LUF5505) or above 1.35 (LUF5521, IBMECA to LUF5595, LUF5589, MRS7140, MRS5980, and MRS7154 to MRS5667) were selected for further kinetic profiling.

3.4. Binding kinetics of selected hA$_3$ receptor agonists using the competition association assay

Next, the kinetic binding parameters of selected agonists that had either low or high KRI values were determined using the competition association assay with [3H]PSB-11. Association rate constants varied by only 11-fold, ranging from (8.8 ± 1.4) × 10^4 M^{-1} s^{-1} for LUF5505 to (9.6 ± 3.1) × 10^5 M^{-1} s^{-1} for LUF5595 (Tables 2 and 3). There was a more pronounced 188-fold difference in dissociation rate constants, in line with the divergent KRI values (LUF5501: (1.6 ± 0.2) × 10^{-3} s^{-1} vs MRS5698: (8.5 ± 0.7) × 10^{-6} s^{-1}). The shortest RT agonist, LUF5501, presented a gradually ascending curve in the competition association assays (Fig. 2A). Of note, the dissociation of MRS5679, with the largest KRI value (5.56), was determined as very slow and not readily quantitated under the current method. The very prominent "overshoot" in the competition association curve was already indicative of a much slower dissociation rate than [3H]PSB-11 (Fig. 2B). Notably, a significant correlation between the negative logarithm of the dissociation rate constants for the selected agonists and their KRI values derived from the kinetic assays was obtained (Fig. 3A), which confirmed that a compound's KRI value is a good predictor for its dissociation rate constant. Besides, a significant correlation was also observed between the agonist affinities (pK$_i$ values) determined in equilibrium displacement experiments and their pK$_D$ values ("kinetic K$_D$ values") derived from competition association experiments, although the pK$_D$ values were on average one log unit higher than the pK$_i$ values (Fig. 3B). As to the kinetic rate constants (k$_{on}$ or k$_{off}$) of the hA$_3$ receptor agonists, their association rate constants showed a better correlation with affinity than their dissociation rate constants (Fig. 3C and D). Furthermore, a k$_{on}$-k$_{off}$-K$_D$ "kinetic map" (Fig. 4) was constructed based on the compounds' divergent affinities (expressed as kinetic K$_D$ values) and rate constants, yielding a division of these agonists into three different sub-categories: agonists that show k$_{off}$ values in a lower range but due to divergent k$_{on}$ values have various K$_D$ values (Group
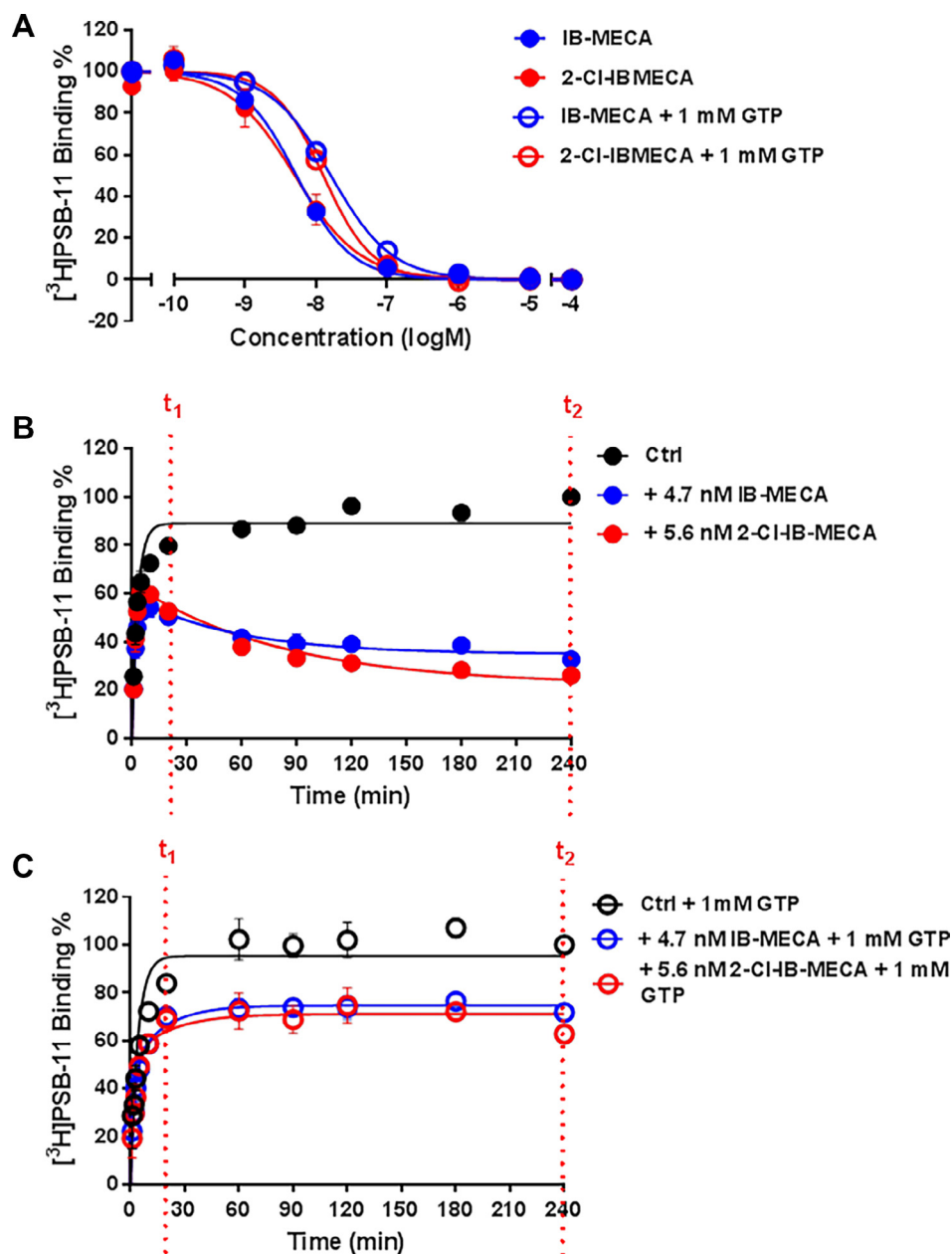
Fig. 1. Displacement of specific [^{3}H]PSB-11 binding from the recombinant hA$_3$ receptor stably expressed on CHO cell membranes by IB-MECA and 2-Cl-IB-MECA in the absence (closed symbols) or presence of 1 mM GTP (open symbols) (A); [^{3}H]PSB-11 competition association experiments in the absence (B) or presence (C) of 1 mM GTP with IB-MECA (blue) or 2-Cl-IB-MECA (red). Combined graphs are shown from at least three experiments performed in duplicate (see Table 1 for pK$_i$ values and kinetic parameters). Note, t$_1$, t$_2$ are indicated, which are the two time points used in KRI determinations.

A); agonists that show k$_{off}$ values in a median range but due to divergent k$_{on}$ values (although smaller than in Group A) have different K$_D$ values (Group B); and two agonists that have relatively poor affinity due to larger k$_{off}$ values and smaller k$_{on}$ values (Group C).

### 3.5. Structure−affinity relationships (SAR) and structure−kinetics relationships (SKR) of hA$_3$ receptor agonists

First, a series of hA$_3$R agonists with either a natural or 5′-modified ribose moiety was investigated (Table 2). LUF5501-LUF5506 have an intact ribofurano moiety and a halogen substitution at the N^6 phenyl group of the core scaffold. 3-Chlorophenyl substitution (LUF5501) provided somewhat better affinity than 3-bromophenyl (LUF5505) or 4-chlorophenyl (LUF5500) substitu-

tion (31 nM vs 78 nM; 31 nM vs 51 nM, respectively). The affinity of the 4-iodophenyl substituted derivative (LUF5506) was similar to LUF5501 (31 nM vs 29 nM). Meanwhile, their KRI values showed that halogen substitution at *meta*-position led to lower KRI values than those at *para*-position of the phenyl ring. The KRI values of LUF5501 and LUF5505 were at the lower end (<0.7) with 0.64 and 0.65, respectively. The full-curve competition association experiments confirmed their similar fast dissociation rates (LUF5501: (1.6 ± 0.2) × 10^{-3} s^{-1}; LUF5505: (1.1 ± 0.04) × 10^{-3} s^{-1}). Worthy of note, LUF5501 proved to have the shortest RT (10 min) among the entire selection of compounds.

When the 5′-hydroxymethylene group (LUF5506) was substituted by an ethylcarboxamide (–CONHCH$_2$CH$_3$, LUF5521), affinity (14 nM vs 29 nM) and particularly the KRI increased (2.06 vs 0.99). The association and dissociation rates of LUF5521 were

Table 2
Binding affinities and kinetic parameters (KRI, k_{on}, k_{off}, RT and K_D) for ribofurano derivatives as hA_3 receptor agonists.
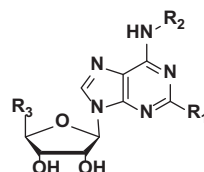
Agonists	R_1	R_2	R_3	pKi (mean K_i in nM)[a]	KRI[b]	k_{on} (M^{-1} s^{-1})[c]	k_{off} (s^{-1})[d]	RT (min)[e]	Kinetic K_D (mean pK_D)[f]
LUF5501	H	–Ph-3-Cl	–CH_2OH	7.5 ± 0.02 (31)	0.64 (0.53; 0.75)	$(1.7 ± 0.2) × 10^5$	$(1.6 ± 0.2) × 10^{-3}$	10 ± 1.3	9.2 ± 1.4 (8.0)
LUF5505	H	–Ph-3-Br	–CH_2OH	7.1 ± 0.1 (78)	0.65 (0.63; 0.66)	$(8.8 ± 1.4) × 10^4$	$(1.1 ± 0.04) × 10^{-3}$	16 ± 0.6	12 ± 1.9 (7.9)
LUF5500	H	–Ph-4-Cl	–CH_2OH	7.3 ± 0.03 (51)	0.98 (0.95; 1.01)	N.D.[h]	N.D.	N.D.	N.D.
LUF5506	H	–Ph-4-I	–CH_2OH	7.6 ± 0.08 (29)	0.99 (0.98; 1.00)	N.D.	N.D.	N.D.	N.D.
LUF5521	H	–Ph-4-I	–$CONHCH_2CH_3$	7.9 ± 0.06 (14)	2.06 ± 0.82	$(1.9 ± 0.3) × 10^5$	$(1.4 ± 0.1) × 10^{-4}$	117 ± 12	0.76 ± 0.13 (9.1)
MECA	H	–CH_2Ph	–$CONHCH_3$	7.4 ± 0.04 (42)	1.24 ± 0.09	N.D.	N.D.	N.D.	N.D.
IB-MECA[g]	H	–CH_2Ph-3-I	–$CONHCH_3$	8.5 ± 0.07 (2.9)	1.55 ± 0.07	$(5.9 ± 0.9) × 10^5$	$(1.8 ± 0.2) × 10^{-4}$	95 ± 13	0.30 ± 0.06 (9.5)
2-Cl-IB-MECA[g]	–Cl	–CH_2Ph-3-I	–$CONHCH_3$	8.5 ± 0.1 (3.5)	2.02 ± 0.06	$(4.0 ± 0.5) × 10^5$	$(7.2 ± 1.1) × 10^{-5}$	231 ± 34	0.18 ± 0.04 (9.7)
LUF5595	–Cl	-CH_2Ph-3-I	-$CH_2OC_3H_5$	8.5 ± 0.09 (3.2)	1.37 (1.39; 1.35)	$(9.6 ± 3.1) × 10^5$	$(2.3 ± 1.0) × 10^{-4}$	72 ± 30	0.24 ± 0.13 (9.6)
LUF5586	H	–CH_2Ph-3-I	–$CH_2OCH_2CH_3$	8.6 ± 0.04 (2.8)	1.30 (1.30; 1.29)	N.D.	N.D.	N.D.	N.D.
LUF5589	–Cl	–CH_2Ph-3-I	–$CH_2OCH_2CH_3$	8.7 ± 0.08 (2.2)	1.66 ± 0.21	$(8.4 ± 0.7) × 10^5$	$(1.2 ± 0.3) × 10^{-4}$	138 ± 37	0.14 ± 0.04 (9.8)
MRS7294	–C≡C-C_4H_2S-5-Cl	–CH_3	–CH_2OH	8.4 ± 0.05 (3.7)	1.63 (1.50; 1.75)	$(8.2 ± 3.8) × 10^5$	$(1.3 ± 0.2) × 10^{-4}$	125 ± 14	0.16 ± 0.02 (9.8)

[a] pKi ± SEM (n ≥ 3, mean K_i value in nM), obtained from radioligand binding assays with [³H]PSB-11 on the hA_3 receptor stably expressed on CHO cell membranes.

[b] KRI ± SEM (n = 3) or KRI (n1,n2) (n = 2), obtained from dual-point competition association assays with [³H]PSB-11 on the hA_3 receptor stably expressed on CHO cell membranes.

[c] k_{on} ± SEM (n ≥ 3), obtained from competition association assays with [³H]PSB-11 on the hA_3 receptor stably expressed on CHO cell membranes.

[d] k_{off} ± SEM (n ≥ 3), obtained from competition association assays with [³H]PSB-11 on the hA_3 receptor stably expressed on CHO cell membranes.

[e] RT = $1/(60 * k_{off})$; RT is expressed in min, whereas k_{off} is expressed in s^{-1}.

[f] $K_D = k_{off}/k_{on}$, expressed in nM

[g] Values taken from Table 1.

[h] N.D. = not determined.

Table 3
Binding affinities and kinetic parameters (KRI, k_{on}, k_{off}, RT and K_D) for (N)-methanocarba derivatives as hA_3 receptor agonists.
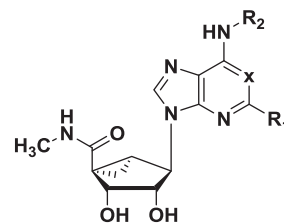
Agonists	X	R_1	R_2	pKi (mean K_i value in nM) [a]	KRI [b]	k_{on} (M^{-1} s^{-1}) [c]	k_{off} (s^{-1}) [d]	RT (min) [e]	Kinetic K_D (mean pK$_D$)[f]
MRS7294 [g]	N	—C≡C-C$_4$H$_2$S-5-Cl	–CH$_3$	8.4 ± 0.05 (3.7)	1.63 (1.50; 1.75)	(8.2 ± 3.8) ×10^5	(1.3 ± 0.2) ×10^{-4}	125 ± 14	0.16 ± 0.02 (9.8)
MRS5980	N	—C≡C-C$_4$H$_2$S-5-Cl	–CH$_3$	9.2 ± 0.09 (0.72)	1.97 (1.87; 2.06)	(9.0 ± 2.3) ×10^5	(4.0 ± 1.0) ×10^{-5}	417 ± 104	0.044 ± 0.016 (10.4)
MRS7140	C	—C≡C-C$_4$H$_2$S-5-Cl	–CH$_3$	8.3 ± 0.08 (5.2)	1.94 (1.82; 2.07)	(3.2 ± 1.2) ×10^5	(8.5 ± 0.3) ×10^{-5}	196 ± 8	0.27 ± 0.10 (9.6)
MRS7154	N	—C≡C-C$_4$H$_2$S-5-Cl	–CH$_2$CH$_2$CH$_3$	8.7 ± 0.06 (2.2)	1.67 (1.75; 1.59)	(4.0 ± 0.7) ×10^5	(6.2 ± 1.2) ×10^{-5}	270 ± 51	0.15 ± 0.04 (9.8)
MRS3558	N	—Cl	-CH$_2$Ph-3-Cl	9.1 ± 0.2 (1.0)	1.49 (1.33; 1.64)	(5.7 ± 0.8) ×10^5	(1.0 ± 0.2) ×10^{-4}	167 ± 39	0.18 ± 0.05 (9.8)
MRS5655	N	—C≡C-Ph	-CH$_2$Ph-3-Cl	8.5 ± 0.09 (3.6)	2.58 (2.05; 3.12)	(4.0 ± 0.8) ×10^5	(1.8 ± 0.3) ×10^{-5}	909 ± 165	0.046 ± 0.013 (10.3)
MRS5644	N	—C≡C-Ph	–CH$_3$	8.6 ± 0.01 (2.4)	2.42 (2.28; 2.56)	(4.5 ± 1.8) ×10^5	(1.4 ± 0.2) ×10^{-5}	1205 ± 174	0.031 ± 0.013 (10.5)
MRS5698	N	-C≡C-(3,4-di-F-Ph)	-CH$_2$Ph-3-Cl	8.1 ± 0.2 (9.4)	4.21 (3.75; 4.67)	(1.3 ± 0.4) ×10^5	(8.5 ± 0.7) ×10^{-6}	1961 ± 154	0.068 ± 0.020 (10.2)
MRS5679	N	—C≡C-(4-biphenyl)	-CH$_2$Ph-3-Cl	7.1 ± 0.05 (82)	5.56 (6.00; 5.11)	undefined	undefined	undefined	undefined
MRS5667	N	—C≡C-(4-biphenyl)	–CH$_3$	8.3 ± 0.05 (4.6)	3.34 (3.14; 3.55)	(1.8 ± 0.3) ×10^5	(1.1 ± 0.3) ×10^{-5}	1563 ± 464	0.058 ± 0.020 (10.2)

[a] pKi ± SEM (n ≥ 3, mean K_i value in nM), obtained from radioligand binding assays with [^{3}H]PSB-11 on the hA_3 receptor stably expressed on CHO cell membranes.
[b] KRI ± SEM (n = 3) or KRI (n1,n2) (n = 2), obtained from dual-point competition association assays with [^{3}H]PSB-11 on the hA_3 receptor stably expressed on CHO cell membranes.
[c] k_{on} ± SEM (n ≥ 3), obtained from competition association assays with [^{3}H]PSB-11 on the hA_3 receptor stably expressed on CHO cell membranes.
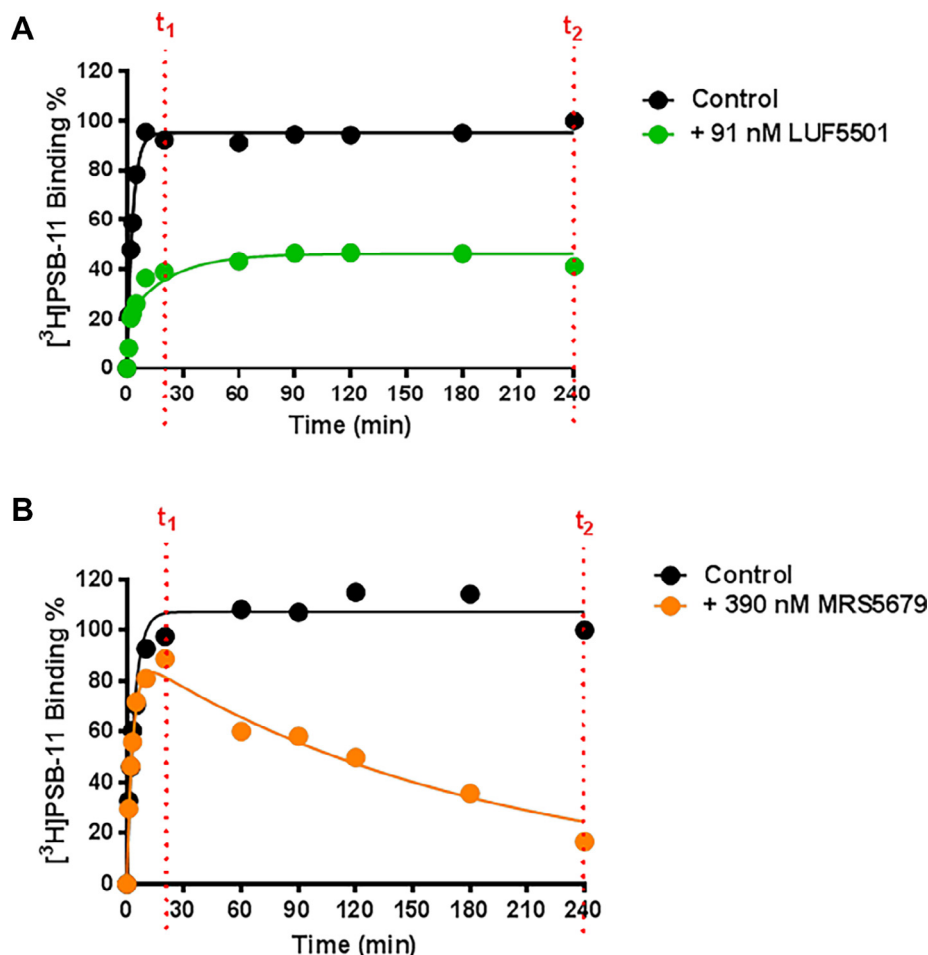[d] k_{off} ± SEM (n ≥ 3), obtained from competition association assays with [^{3}H]PSB-11 on the hA_3 receptor stably expressed on CHO cell membranes.
[e] RT = 1/(60 * k_{off}); RT is expressed in min, whereas k_{off} is expressed in s^{-1}.
[f] K_D = k_{off}/k_{on}, expressed in nM.
[g] MRS7294 has a ribofurano ring (see also Table 2).

Fig. 2. Competition association experiments with [³H]PSB-11 binding to the recombinant hA₃ receptor stably expressed on CHO cell membranes (10 °C) in the absence or presence of unlabeled short-residence-time agonist LUF5501 (A), or long-residence-time agonist MRS5679 (B). Representative graphs are shown from one experiment performed in duplicate. Note, t_1, t_2 are indicated, which are the two time points used in KRI determinations.

$(1.9 \pm 0.3) \times 10^5 \, M^{-1} \, s^{-1}$ and $(1.4 \pm 0.1) \times 10^{-4} \, s^{-1}$, respectively, and its RT was calculated as 117 min.
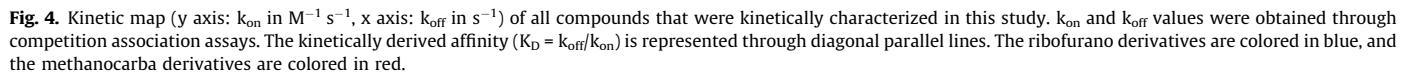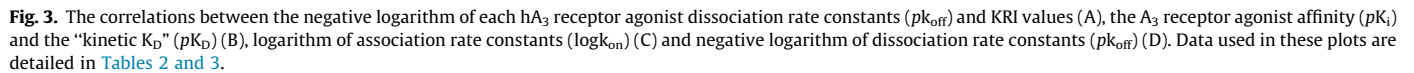
We then examined benzyl substitutions at the N^6 position of the core scaffold, with a methylcarboxamide (–CONHCH₃) modification of the 5′-position on the ribofuran moiety (MECA, IB-MECA and 2-Cl-IBMECA). MECA had an affinity of 42 nM with a KRI value of 1.24. When iodine was introduced at the 3-position of the benzyl ring, yielding IB-MECA, affinity was strongly increased (2.9 nM vs 42 nM) as well as the KRI value (1.55 vs 1.24); with a further chlorine atom substitution at the C-2 position on the core scaffold (2-Cl-IBMECA) there was no further increase in affinity (3.5 nM vs 2.9 nM), but its KRI value increased significantly (2.02 vs 1.55), which is the largest value in this series (Table 2). For IB-MECA and 2-Cl-IBMECA, the association rate constants were similar ((5.9 ± 0.9) × $10^5 \, M^{-1} \, s^{-1}$ vs $(4.0 \pm 0.5) \times 10^5 \, M^{-1} \, s^{-1}$), however 2-Cl-IBMECA had a slower dissociation rate ($(7.2 \pm 1.1) \times 10^{-5} \, s^{-1}$ vs $(1.8 \pm 0.2) \times 10^{-4} \, s^{-1}$) as had been immanent already from their KRI values. The RTs of IB-MECA and 2-Cl-IBMECA were calculated from their dissociation rate constants as 95 min and 231 min, respectively.

Interestingly, when the amide at the 5′-position on the ribofurano ring of 2-Cl-IBMECA was changed to an ether function (–CH₂-OC₃H₅, **LUF5595**), both association ($(9.6 \pm 3.1) \times 10^5 \, M^{-1} \, s^{-1}$ vs $(4.0 \pm 0.5) \times 10^5 \, M^{-1} \, s^{-1}$) and dissociation ($(2.3 \pm 1.0) \times 10^{-4} \, s^{-1}$ vs $(7.2 \pm 1.1) \times 10^{-5} \, s^{-1}$) became faster, even though the compound was still a slowly dissociating agonist compared with the radioligand (KRI: 1.37).

Finally, the effect of the 2-Cl substitution was further confirmed in the comparison between **LUF5586** and **LUF5589**. Their affinities were similar (2.8 nM vs 2.2 nM), but with 2-Cl, **LUF5589** had a higher KRI than **LUF5586** (1.66 vs 1.30), and the RT of **LUF5589** was determined as 138 min. In addition, a larger substituent at the C-2 position (**MRS7294**) was tolerated with respect to both affinity and kinetics, at least in combination with a small N^6-methyl substituent.

Table 3 summarizes our findings on the series of ring-rigidified methanocarba derivatives that maintain a receptor-preferred North (N) conformation, with the flexible ribose-substituted MRS7294 included once more to allow a comparison. MRS7294, MRS5980, MRS7140, MRS7158 and MRS7154 share a common fragment ((5-chlorothiophen-2-yl)ethynyl) at the C-2-position (R₁ group). MRS7294, the agonist with unmodified ribofuran moiety, served as the starting of the analysis, which had both high affinity (3.7 nM) and a large KRI value (1.63). By competition association experiments its association and dissociation rates were determined as $(8.2 \pm 3.8) \times 10^5 \, (M^{-1} \, s^{-1})$ and $(1.3 \pm 0.2) \times 10^{-4} \, s^{-1}$, respectively; its RT was calculated as 125 min. When the ribofurano ring was changed by the methanocarba moiety (MRS5980), the affinity increased to the sub-nanomolar range (0.72 nM vs 3.7 nM) and its KRI value also increased largely (1.97 vs 1.63). The full-curve competition association experiments showed that MRS5980's association rate was slightly faster ($(9.0 \pm 2.3) \times 10^5 \, M^{-1} \, s^{-1}$ vs $(8.2 \pm 3.8) \times 10^5 \, M^{-1} \, s^{-1}$ for the respective rate

Fig. 3. The correlations between the negative logarithm of each hA_3 receptor agonist dissociation rate constants (pk_{off}) and KRI values (A), the A_3 receptor agonist affinity (pK_i) and the "kinetic K_D" (pK_D) (B), logarithm of association rate constants ($logk_{on}$) (C) and negative logarithm of dissociation rate constants (pk_{off}) (D). Data used in these plots are detailed in Tables 2 and 3.

Fig. 4. Kinetic map (y axis: k_{on} in $M^{-1} s^{-1}$, x axis: k_{off} in s^{-1}) of all compounds that were kinetically characterized in this study. k_{on} and k_{off} values were obtained through competition association assays. The kinetically derived affinity ($K_D = k_{off}/k_{on}$) is represented through diagonal parallel lines. The ribofurano derivatives are colored in blue, and the methanocarba derivatives are colored in red.

constants), but its dissociation rate was much slower (($4.0 \pm 1.0) \times 10^{-5} s^{-1}$ vs ($1.3 \pm 0.2) \times 10^{-4} s^{-1}$) than its ribose-equivalent. The RT of MRS5980 was 417 min. When the nitrogen atom at the N-1-position was replaced by a carbon atom (MRS7140), the affinity remained high (5.2 nM), and its kinetics profile was not much altered compared with MRS5980 (k_{on}: ($3.2 \pm 1.2) \times 10^5 M^{-1} s^{-1}$ vs ($9.0 \pm 2.3) \times 10^5 M^{-1} s^{-1}$; k_{off}: ($8.5 \pm 0.3) \times 10^{-5} s^{-1}$ vs ($4.0 \pm$

$1.0) \times 10^{-5} s^{-1}$). Changing the mono-methyl substitution at the N^6 position (MRS5980) for di-methyl substitution (MRS7158), severely compromised both affinity and KRI value (618 nM vs 0.72 nM; 0.93 vs 1.97). When mono-substitution at the N^6 position (MRS7140) was extended to n-propyl (MRS7154), affinity remained high (2.2 nM), like the KRI value (1.67); both association and dissociation rates of MRS7154 were quite similar to MRS5980

(k_{on}: $(4.0 \pm 0.7) \times 10^5 \, M^{-1} \, s^{-1}$ vs $(9.0 \pm 2.3) \times 10^5 \, M^{-1} \, s^{-1}$; k_{off}: $(6.2 \pm 1.2) \times 10^{-5} \, s^{-1}$ vs $(4.0 \pm 1.0) \times 10^{-5} \, s^{-1}$), with RTs of 270 min and 417 min, respectively.

The methanocarba derivatives MRS3558, MRS5655, MRS5679 and MRS5698 share their R_2 groups (3-chlorobenzyl substitution). When the 2-Cl substituent of MRS3558 was replaced by the bulky and rigid phenylethynyl (MRS5655), the affinity decreased from 1.0 nM (MRS3558) to 3.6 nM (MRS5655), while the KRI value increased, however (1.49 vs 2.58). In the competition association assays the association rate constants of MRS3558 and MRS5655 were similar ($(5.7 \pm 0.8) \times 10^5 \, M^{-1} \, s^{-1}$ vs $(4.0 \pm 0.8) \times 10^5 \, M^{-1} \, s^{-1}$), while the dissociation rate constants were 5.6-fold different ($(1.0 \pm 0.2) \times 10^{-4} \, s^{-1}$ vs $(1.8 \pm 0.3) \times 10^{-5} \, s^{-1}$), leading to a RT for MRS5655 of 909 min. When the phenylethynyl of MRS5655 was 3,4-di-fluorinated as in MRS5698, the affinity was reduced from 3.6 nM (MRS5655) to 9.4 nM (MRS5698), while the KRI value increased significantly from 2.58 (MRS5655) to 4.21 (MRS5698), with both slower association and dissociation rate constants (k_{on}: $(4.0 \pm 0.8) \times 10^5 \, M^{-1} \, s^{-1}$ vs $(1.3 \pm 0.4) \times 10^5 \, M^{-1} \, s^{-1}$; k_{off}: $(1.8 \pm 0.3) \times 10^{-5} \, s^{-1}$ vs $(8.5 \pm 0.7) \times 10^{-6} \, s^{-1}$), thus extending RT from 909 min to 1961 min. Furthermore, when the phenylethynyl fragment of MRS5655 was expanded to a 4-biphenylethynyl substitution on the R_1 group (MRS5679), the affinity suffered from 3.6 nM (MRS5655) to 82 nM (MRS5679); however, its KRI value increased dramatically from 2.58 to 5.56. This high value rendered the determination of the kinetics profile of MRS5679 impossible. Obviously, from all these compounds we learned there can be a clear dichotomy between affinity and residence time.

When the benzyl substitutions at the N^6 position (R_2 in Table 3) were replaced by a simple monomethyl (i.e. MRS5655 to MRS5644; MRS5679 to MRS5667), their binding affinities to hA$_3$ receptors were not compromised (MRS5655/MRS5644: 3.6 nM vs 2.4 nM) or even increased (MRS5679/MRS5667: 82 nM vs 4.6 nM), and so were the kinetics profiles of MRS5655 and MRS5644. The KRI values of MRS5679 and MRS5667 were both at the higher end (5.56 and 3.34).

4. Discussion

4.1. Effects of GTP on agonist binding to the human adenosine A₃ receptor

In the current study, the binding interactions of unlabeled hA$_3$ receptor agonists were determined in radioligand binding experiments with the reference tritiated antagonist [3H]PSB-11. The favorable binding characteristics of this radioligand served us particularly well in the competition association experiments where robust binding over time could still be measured in the presence of unlabeled ligands, essential for the calculation of the association and dissociation rate constants. It is well known that antagonists occupy a GPCR irrespective of whether it is coupled to a G protein, whereas agonists prefer the G protein-coupled state of the receptor [36]. Addition of GTP to the incubation mixture induces an uncoupling between receptor and available G protein, which leads to a lower apparent receptor affinity for agonists. We confirmed this behavior in our equilibrium displacement experiments, in which the two reference agonists IB-MECA and 2-Cl-IB-MECA had a 3–4-fold lower affinity in the presence of GTP (Fig. 1A, Table 1). Interestingly, all displacement curves had pseudo-Hill coefficients of approx. unity (Table 1), suggesting that the agonists recognized one receptor state in both the presence and absence of GTP, most likely a G protein-coupled state (no GTP) or an uncoupled state (with GTP). We then determined the agonist binding kinetics for the two states in subsequent competition association assays by measuring these in the absence or presence of GTP (Fig. 1B). Inter-

estingly, the association rate constants were identical for the two states (Table 1). Apparently, the ligand, when approaching the receptor from the extracellular side, is insensitive to the coupling status at the intracellular G protein interface. However, the dissociation kinetics proved to be (significantly) different between the states, up to 8-fold for 2-Cl-IB-MECA (Table 1), suggesting that dissociating from the receptor is influenced by the absence or presence of the G protein. We then performed further experiments in the absence of GTP, as we felt that for the case of the hA$_3$ receptor this experimental condition provides us information on the more relevant high-affinity agonist binding state of the receptor. The mathematical modeling provided by Motulsky and Mahan [32] does not allow the calculation of two receptor states with corresponding kinetic parameters. Hence, in a number of cases similar to ours it was decided to include GTP in the assays. For the adenosine A$_1$ receptor, we included GTP in our assays, forcing the receptor to be in one lower affinity, G protein-uncoupled state only; with this restriction, the kinetic parameters of agonists were determined as conveniently as antagonists [37]. Likewise, the team of Charlton included GTP in kinetic assays on the muscarinic M$_3$ receptor [38]. On the other hand, GTP was excluded in assays on the adenosine A$_{2A}$ receptor, as agonist affinity at this protein is insensitive to GTP in both equilibrium and kinetics assays [39].

4.2. Methodological aspects of the radioligand binding assays

To ensure an accurate and robust kinetic quantification, experiments were performed at 10 °C, as reported and documented previously [35]. Initially, a so-called dual-point competition association assay yielding KRI values for the hA$_3$ receptor was performed as a "kinetic screening campaign" to increase throughput in comparison to the traditional, more elaborate, competition association experiments [35]. Although fast kinetics of agonist binding (e.g. LUF5501, Fig. 2A) was determined accurately at a relatively low temperature, the kinetics of one agonist with obviously very slow dissociation characteristics (MRS5679, Fig. 2B) could not be reliably determined with the Motulsky-Mahan equations. Meanwhile, its large KRI value (5.56) undoubtedly reflects its slow dissociation.

Besides the significant correlation between the agonists' KRI values and dissociation rate constants (Fig. 3A), the equilibrium K$_i$ and kinetic K$_D$ values were also well correlated (Fig. 3B). Despite this correlation there are large discrepancies in values between the equilibrium affinities (K$_i$) and kinetic K$_D$ values. In general, the kinetic pK$_D$ values are higher than pK$_i$ values, with differences from 0.5 to 2.1 log-unit (LUF5501 and MRS5698), while the short RT agonists have smaller differences than long RT agonists. This phenomenon suggests that the affinities determined in the radioligand displacement studies may not reflect the true affinity of the compounds as many of them have residence times much longer than the (already long) incubation time of 240 min. In fact, this points to a general caveat in end-point assays in which the equilibrium characteristics of the probe, e.g., a radiolabeled or fluorescently tagged compound, determine the assay protocol without further consideration of the same characteristics of the unlabeled ligands to be tested.

Furthermore, there was a significant correlation between k_{on} (k_3) and affinity values (K$_i$) of the agonists, but no relationship was found between k_{off} (k_4) and K$_i$ (Fig. 3C and D). Such correlation between affinity and on-rates has been reported in the case of other GPCRs [40] and ion channels [41,42]. However, in the current study, variations in association rate constants were approximately 10-fold (logk_{on}: 5.0–6.0), much smaller than at the other targets mentioned above. In addition, all the association rates were well below the diffusion limit of around $10^7 \, M^{-1} \, s^{-1}$, which had been observed previously for membrane-bound proteins [43].

4.3. Ligand optimization based on structure−kinetics relationships (SKRs)

All the agonists examined in the current study have been reported, and the riboside MRS7294 was most recently disclosed as a hA$_3$ receptor agonist [28]. Most ribofurano derivatives (Table 2) had been synthesized and tested as early as 1994 [44]. The (N)-methanocarba derivatives (Table 3) were explored more recently, showing generally improved affinities over the earlier compounds [26–29]. Although most of these compounds have been described in the context of structure-affinity relationships (SAR), we reasoned that an extensive structure–kinetics relationships (SKR) analysis is warranted since kinetic profiles are emerging indicators of *in vivo* functional efficacy [18,20,21,45].

In the series of ribofurano derivatives (Table 2), the most outstanding agonist with respect to residence time was 2-Cl-IB-MECA (231 min). The underlying chemical features that prolonged the residence time in the ribofurano series are: i) a chlorine atom at the C2 position (R$_1$ in Table 2, IB-MECA vs 2-Cl-IB-MECA, 95 min vs 231 min; LUF5586 vs LUF5589 in KRI: 1.30 vs 1.66), ii) a bulky *meta*-iodobenzyl substitution at the N^6 position of the adenine nucleobase (R$_2$ in Table 2, MECA vs IB-MECA in KRI: 1.24 vs 1.55), and iii) an amide modification at the 5′ position (R$_3$ in Table 2, 2-Cl-IB-MECA vs LUF5595: 231 min vs 72 min; LUF5506 vs LUF5521 in KRI: 0.99 vs 2.06). Interestingly, slow dissociation kinetics of agonists can be maintained by introducing an extended linear side chain at the C2 position and removing the bulky substituent at the N^6 position (i.e. N^6-Me analogue MRS7294 in RT: 125 min). The kinetic behavior of another known reference agonist, 2-(1-hexynyl)-N-methyladenosine (HEMADO), also confirmed this observation from comparison with other research [45,46].

More impressive kinetics were observed in the methanocarba series. From a previous study it was concluded that a possible H-bond interaction between the amide modification at the original 5′ position (–CONHCH$_3$) and residues in the binding pocket of the hA$_3$ receptor was a key feature of agonist kinetics [47]. Comparing the kinetics of ribofurano MRS7294 and its methanocarba equivalent MRS5980 provides evidence the conformational-constrained (N)-methanocarba moiety as a ribofurano ring substitute adds to the slow dissociation of MRS5980, suggesting this rigid ring system fits even better in the ligand binding pocket. Additionally, the N1 atom on the adenine core is contributing to slow dissociation (1-deza MRS7140 vs MRS5980 in RT: 196 min vs 417 min). The N^6 position in the methanocarba series (R$_2$ substituent) accepted a small methyl group as avidly as the larger *n*-propyl (MRS5980 vs MRS7154) and 3-chlorobenzyl substituent (MRS5644 vs MRS5655), with respect to both affinity and kinetics. Apparently, differences in lipophilicity between the N^6-substituents did not seem to matter either. Data for the R$_1$ (C2 position) substituent were already commented on in the Results section. It is noteworthy that the 3,4-difluorophenyl fragment contributed to a long residence time of MRS5698, quite similar to the 2,4-difluorophenyl fragment we encountered in A$_{2A}$ receptor antagonists displaying long residence time [48].

So far the human A$_3$ receptor has not been crystallized yet, although its most homologous relative, the adenosine A$_1$ receptor, has [49]. Homology models of the A$_3$ receptor have been constructed, and their relevance has been recently reviewed and discussed [50]. It appeared that the interaction of the extended and rigid 2-arylethynyl groups at the C-2 position (as in e.g., MRS5679 and MRS5644) with the A$_3$ receptor required an outward movement of TM2. Although the agonists' path of binding to or dissociation from the A$_3$ receptor is unknown, one could speculate that such reorganization of TM2 "locks" the C2-substituted agonist. This reasoning stems from a molecular dynamics simulation and site-directed mutation study of the ligand dissociation pathway from the human adenosine A$_{2A}$ receptor [51], for which we used a high resolution crystal structure [52]. It taught us there may be a lid adjacent to the ligand binding pocket retaining the ligand for some time before the compound leaves the receptor. A follow-up study revealed that ligand dissociation correlated with the strength of the salt-bridge between His264 in EL3 and Glu169 in EL2 [53]. It would be interesting to learn whether a similar mechanism exists for the A$_3$ receptor.

4.4. Retrospective evaluation of selected agonists with complete kinetic profiles

IB-MECA (RT = 95 min) and 2-Cl-IB-MECA (RT = 231 min) are two reference full agonists for the hA$_3$ receptor. Despite numerous reports about their controversial cardioprotection [54,55], they have been taken into a series of clinical trials: for IB-MECA, in total 12 completed or planned trials have been reported related to inflammatory conditions (e.g., keratoconjunctivitis sicca, rheumatoid arthritis, psoriasis, uveitis); for 2-Cl-IB-MECA, four trials have been registered for liver diseases (e.g., hepatocellular carcinoma, hepatitis C) [56,57]. Intuitively one would expect that long residence time hA$_3$ receptor agonists could be beneficial in chronic diseases, for instance to allow once daily dosing.

More recently, the neuroprotective effect provided by hA$_3$ receptor agonists has been receiving attention [11,58]. A number of agonists have been designed and evaluated both in *in vitro* and *in vivo* functional experiments, especially for the treatment of chronic neuropathic pain [26,27,29]. MRS5698 in particular, having the longest residence time (1961 min) from our research, has been studied extensively in various pre-clinical animal models of neuropathic pain [59–61]. We, however, hesitate to link the binding kinetics profile of MRS5698 with its *in vivo* effects, also because issues such as pharmacokinetics and species differences (human/rodent) may play an important but yet unknown role.

The adenosine A$_3$ receptor has a peculiar and rapid desensitization/internalization profile in cultured cells [6]. However, the fast desensitization after A$_3$ agonist exposure under *in vitro* conditions does not generalize to *in vivo* pain models. MRS5698 maintained full efficacy over a five-day period, with the drug administered either by daily injection or by an implanted mini-pump to provide a steady state plasma concentration [55]. Prolonged MRS5698 exposure in the rat did not reduce its efficacy, as would be expected from agonist-induced desensitization alone. Thus, additional studies of agonist occupancy of the receptor and subsequent receptor processing are warranted to further explore this interesting target for combatting neuropathic pain.

4.5. Kinetic map

Using the association (k_{on}) and dissociation (k_{off}) rate constants obtained from competition association experiments (Tables 2 and 3), a kinetic map (Fig. 4) was constructed by plotting these values on the y-axis and x-axis, respectively. The dashed diagonal parallel lines represent the kinetically derived K$_D$ values (K$_D$ = k_{off}/k_{on}). Out of this map three subgroups emerged, which were divided according to k_{off} values: Group A < Group B < Group C. Obviously, Groups A and C are solely composed of methanocarba derivatives (Fig. 4, red) and ribofurano derivatives (Fig. 4, blue), respectively. Group B is a mixture of these two compound classes, with the methanocarba derivatives mainly displaying smaller k_{off} values. Thus, rigidifying the ribose ring with the bicyclic group consistently prolonged the dissociation time. This general division indicates a different mode of receptor-ligand interaction during the binding and unbinding process of the two ligand groups. It also seems there is a clear residence-time "cliff" between Groups A (having one rigid C2-phenylethynyl or 4-biphenylethynyl group with or without one

enlarged N^6-benzyl group) and B (having multiple enlarged adenine substituents) in the kinetic map.

In each subgroup, agonists exhibit k_{off} values in a similar range, but have different k_{on} values. As a consequence, variation in K_D values in each group was observed (Group A: ~10-fold; Group B: ~100-fold; Group C: ~3-fold). Previous SKR studies have primarily focused on optimizing dissociation rates and residence times for designing a kinetically favorable ligand. Yet recently, there has been increasing acknowledgement of the important role association rate constants may play in determining the efficacy of a drug as the result of increased rebinding or increased drug-target selectivity [21,62]. A kinetic map would thus allow for the selection of compounds with appropriate residence times while exploring the role of association rate constants.

In summary, an agonist-related competition association assay at the hA$_3$ receptor was validated, and a series of ribofurano and methanocarba derivatives were kinetically profiled for the first time. A k_{on}-k_{off}-K_D kinetic map was constructed and subsequently the agonists with complete kinetic profile were divided into three subgroups based on their residence times. Longer residence times were associated with methanocarba (vs. ribose) and enlarged adenine N^6 and C-2 (rigid arylalkynyl) substitutions. We identified agonists with very long residence times, but these may not be the most therapeutically favorable for treating various conditions in view of the fast desensitization of the receptor. Although far from definitive, this study suggests that proper residence times, not necessarily longer than target turnover time, may be vital parameters in the development of hA$_3$R agonists for therapeutic use.

Conflict of interest

None.

List of author contributions

Participated in research design; Xia, IJzerman, Heitman.
Conducted experiments; Xia, Kyrizaki, van Duijl, Roorda.
Performed data analysis; Xia, Kyrizaki, van Duijl.
Wrote or contributed to the writing of the manuscript; Xia, Tosh, Jacobson, IJzerman.

Acknowledgements

References

[1] W. Meyerhof, R. Müller-Brechlin, D. Richter, Molecular cloning of a novel putative G-protein coupled receptor expressed during rat spermiogenesis, FEBS Lett. 284 (2) (1991) 155–160.

[2] D. Cortés, R. Guinzberg, R. Villalobos-Molina, E. Piña, Evidence that endogenous inosine and adenosine-mediated hyperglycaemia during ischaemia–reperfusion through A$_3$ adenosine receptors, Auton. Autacoid Pharmacol. 29 (4) (2009) 157–164.

[3] L. Madi, A. Ochaion, L. Rath-Wolfson, S. Bar-Yehuda, A. Erlanger, G. Ohana, A. Harish, O. Merimski, F. Barer, P. Fishman, The A$_3$ adenosine receptor is highly expressed in tumor versus normal cells: potential target for tumor growth inhibition, Clin. Cancer Res. 10 (13) (2004) 4472–4479.

[4] A. Ochaion, S. Bar-Yehuda, S. Cohen, F. Barer, R. Patoka, H. Amital, T. Reitblat, A. Reitblat, J. Ophir, I. Konfino, Y. Chowers, S. Ben-Horin, P. Fishman, The anti-inflammatory target A$_3$ adenosine receptor is over-expressed in rheumatoid arthritis, psoriasis and Crohn's disease, Cell. Immunol. 258 (2) (2009) 115–122.

[5] T.M. Palmer, G.L. Stiles, Identification of threonine residues controlling the agonist-dependent phosphorylation and desensitization of the rat A$_3$ adenosine receptor, Mol. Pharmacol. 57 (3) (2000) 539–545.

[6] E.C. Klaasse, A.P. IJzerman, W.J. de Grip, M.W. Beukers, Internalization and desensitization of adenosine receptors, Purinergic Signalling 4 (1) (2008) 21–37.

[7] S. Gessi, S. Merighi, K. Varani, E. Leung, S. Mac Lennan, P.A. Borea, The A$_3$ adenosine receptor: an enigmatic player in cell biology, Pharmacol. Ther. 117 (1) (2008) 123–140.

[8] N. Shamama, A.K. Luqman, M.A. Zafar, F.B. Seemi, Adenosine A$_3$ receptor: a promising therapeutic target in cardiovascular disease, Curr. Cardiol. Rev. 12 (1) (2016) 18–26.

[9] P.A. Borea, K. Varani, F. Vincenzi, P.G. Baraldi, M.A. Tabrizi, S. Merighi, S. Gessi, The A$_3$ adenosine receptor: history and perspectives, Pharmacol. Rev. 67 (1) (2015) 74–102.

[10] L. Antonioli, B. Csóka, M. Fornai, R. Colucci, E. Kókai, C. Blandizzi, G. Haskó, Adenosine and inflammation: what's new on the horizon? Drug Discov. Today 19 (8) (2014) 1051–1068.

[11] P. Fishman, S. Bar-Yehuda, B.T. Liang, K.A. Jacobson, Pharmacological and therapeutic effects of A$_3$ adenosine receptor (A3AR) agonists, Drug Discov. Today 17 (7–8) (2012) 359–366.

[12] C.E. Müller, K.A. Jacobson, Recent developments in adenosine receptor ligands and their potential as novel drugs, Biochim. Biophys. Acta Biomembr. 1808 (5) (2011) 1290–1308.

[13] B. Koscsó, B. Csóka, P. Pacher, G. Haskó, Investigational A$_3$ adenosine receptor targeting agents, Expert Opin. Invest. Drugs 20 (6) (2011) 757–768.

[14] D. Salvemini, K.A. Jacobson, Highly selective A$_3$ adenosine receptor agonists relieve chronic neuropathic pain, Expert. Ther. Pat. 27 (8) (2017) 967.

[15] P. Fishman, S. Cohen, The A$_3$ adenosine receptor (A3AR): therapeutic target and predictive biological marker in rheumatoid arthritis, Clin. Rheumatol. 35 (9) (2016) 2359–2362.

[16] S. Cohen, S.M. Stemmer, G. Zozulya, A. Ochaion, R. Patoka, F. Barer, S. Bar-Yehuda, L. Rath-Wolfson, K.A. Jacobson, P. Fishman, CF102 an A$_3$ adenosine receptor agonist mediates anti-tumor and anti-inflammatory effects in the liver, J. Cell. Physiol. 226 (9) (2011) 2438–2447.

[17] K.A. Jacobson, S. Merighi, K. Varani, P.A. Borea, S. Baraldi, M. Aghazadeh Tabrizi, R. Romagnoli, P.G. Baraldi, A. Ciancetta, D.K. Tosh, Z.-G. Gao, S. Gessi, A3 adenosine receptors as modulators of inflammation: from medicinal chemistry to therapy, Med. Res. Rev. doi: 10.1002/med.21456.

[18] D. Guo, J.M. Hillger, A.P. IJzerman, L.H. Heitman, Drug-target residence time—a case for G protein-coupled receptors, Med. Res. Rev. 34 (4) (2014) 856–892.

[19] K.P. Cusack, Y. Wang, M.Z. Hoemann, J. Marjanovic, R.G. Heym, A. Vasudevan, Design strategies to address kinetics of drug binding and residence time, Bioorg. Med. Chem. Lett. 25 (10) (2015) 2019–2027.

[20] R.A. Copeland, D.L. Pompliano, T.D. Meek, Drug-target residence time and its implications for lead optimization, Nat. Rev. Drug Discov. 5 (9) (2006) 730–739.

[21] R.A. Copeland, The drug-target residence time model: a 10-year retrospective, Nat. Rev. Drug Discov. 15 (2) (2016) 87–95.

[22] L.H. Heitman, A. Göblyös, A.M. Zweemer, R. Bakker, T. Mulder-Krieger, J.P.D. van Veldhoven, H. de Vries, J. Brussee, A.P. IJzerman, A series of 2,4-disubstituted quinolines as a new class of allosteric enhancers of the adenosine A$_3$ receptor, J. Med. Chem. 52 (4) (2009) 926–931.

[23] S. Gessi, K. Varani, S. Merighi, A. Morelli, D. Ferrari, E. Leung, P.G. Baraldi, G. Spalluto, P.A. Borea, Pharmacological and biochemical characterization of A$_3$ adenosine receptors in Jurkat T cells, Br. J. Pharmacol. 134 (1) (2001) 116–126.

[24] M. de Zwart, M. de Groote, P.A.M. van der Klein, S. van Dun, R. Bronsing, J.K. von Frijtag, Drabbe Künzel, A.P. IJzerman, Phenyl-substituted N^6-phenyladenosines and N^6-phenyl-5'-N-ethylcarboxamidoadenosines with high activity at human adenosine A$_{2B}$ receptors, Drug Dev. Res. 49 (2) (2000) 85–93.

[25] E.W. van Tilburg, P.A.M. van der Klein, J. von Frijtag, Drabbe, Künzel, M. de, Groote, C. Stannek, A. Lorenzen, A.P. IJzerman, 5'-O-alkyl ethers of N,2-substituted adenosine derivatives: partial agonists for the adenosine A$_1$ and A$_3$ receptors, J. Med. Chem. 44 (18) (2001) 2966–2975.

[26] D.K. Tosh, A. Finley, S. Paoletta, S.M. Moss, Z.-G. Gao, E.T. Gizewski, J.A. Auchampach, D. Salvemini, K.A. Jacobson, In vivo phenotypic screening for treating chronic neuropathic pain: modification of C2-arylethynyl group of conformationally constrained A$_3$ adenosine receptor agonists, J. Med. Chem. 57 (23) (2014) 9901–9914.

[27] D.K. Tosh, S. Crane, Z. Chen, S. Paoletta, Z.-G. Gao, E. Gizewski, J.A. Auchampach, D. Salvemini, K.A. Jacobson, Rigidified A$_3$ adenosine receptor agonists: 1-deazaadenine modification maintains high in vivo efficacy, ACS Med. Chem. Lett. 6 (7) (2015) 804–808.

[28] D.K. Tosh, A. Janowsky, A.J. Eshleman, E. Warnick, Z.-G. Gao, Z. Chen, E. Gizewski, J.A. Auchampach, D. Salvemini, K.A. Jacobson, Scaffold repurposing of nucleosides (adenosine receptor agonists): enhanced activity at the human dopamine and norepinephrine sodium symporters, J. Med. Chem. 60 (7) (2017) 3109–3123.

[29] D.K. Tosh, F. Deflorian, K. Phan, Z.-G. Gao, T.C. Wan, E. Gizewski, J.A. Auchampach, K.A. Jacobson, Structure-guided design of A$_3$ adenosine

receptor-selective nucleosides: combination of 2-arylethynyl and bicyclo [3.1.0]hexane substitutions, J. Med. Chem. 55 (10) (2012) 4847–4860.

[30] S. Tchilibon, B.V. Joshi, S.-K. Kim, H.T. Duong, Z.-G. Gao, K.A. Jacobson, (N)-methanocarba 2, N^6-disubstituted adenine nucleosides as highly potent and selective $_A3$ adenosine receptor agonists, J. Med. Chem. 48 (6) (2005) 1745–1758.

[31] P.K. Smith, R.I. Krohn, G.T. Hermanson, A.K. Mallia, F.H. Gartner, M.D. Provenzano, E.K. Fujimoto, N.M. Goeke, B.J. Olson, D.C. Klenk, Measurement of protein using bicinchoninic acid, Anal. Biochem. 150 (1) (1985) 76–85.

[32] H.J. Motulsky, L.C. Mahan, The kinetics of competitive radioligand binding predicted by the law of mass action, Mol. Pharmacol. 25 (1) (1984) 1–9.

[33] D. Guo, E.J.H. van, Dorp, T. Mulder-Krieger, J.P.D. van Veldhoven, J. Brussee, A. P. IJzerman, L.H. Heitman, Dual-point competition association assay: a fast and high-throughput kinetic screening method for assessing ligand-receptor binding kinetics, J. Biomol Screening 18 (3) (2013) 309–320.

[34] Y.-C. Cheng, W.H. Prusoff, Relationship between the inhibition constant (K_I) and the concentration of inhibitor which causes 50 per cent inhibition (IC_{50}) of an enzymatic reaction, Biochem. Pharmacol. 22 (23) (1973) 3099–3108.

[35] L. Xia, W.A.C. Burger, J.P.D. van Veldhoven, B.J. Kuiper, T.T. van Duijl, E.B. Lenselink, E. Paasman, L.H. Heitman, A.P. IJzerman, Structure–affinity relationships and structure–kinetics relationships of pyrido[2,1-f]purine-2,4-dione derivatives as human adenosine A_3 receptor antagonists, J. Med. Chem. 60 (17) (2017) 7555–7568.

[36] S.R. Sprang, Cell signalling: binding the receptor at both ends, Nature 469 (7329) (2011) 172–173.

[37] L. Xia, H. de Vries, A.P. IJzerman, L.H. Heitman, Scintillation proximity assay (SPA) as a new approach to determine a ligand's kinetic profile. A case in point for the adenosine A_1 receptor, Purinergic Signalling 12 (1) (2016) 115–126.

[38] D.A. Sykes, M.R. Dowling, S.J. Charlton, Exploring the mechanism of agonist efficacy: a relationship between efficacy and agonist dissociation rate at the muscarinic M_3 receptor, Mol. Pharmacol. 76 (3) (2009) 543–551.

[39] D. Guo, T. Mulder-Krieger, A.P. IJzerman, L.H. Heitman, Functional efficacy of adenosine A_{2A} receptor agonists is positively correlated to their receptor residence time, Br. J. Pharmacol. 166 (6) (2012) 1846–1859.

[40] M.L.J. Doornbos, J.M. Cid, J. Haubrich, A. Nunes, J.W. van de Sande, S.C. Vermond, T. Mulder-Krieger, A.A. Trabanco, A. Ahnaou, W.H. Drinkenburg, H. Lavreysen, L.H. Heitman, A.P. IJzerman, G. Tresadern, Discovery and kinetic profiling of 7-aryl-1,2,4-triazolo[4,3-a]pyridines: positive allosteric modulators of the metabotropic glutamate receptor 2, J. Med. Chem. 60 (15) (2017) 6704–6720.

[41] Z. Yu, J.P.D. van Veldhoven, J. Louvel, I.M.E. 't Hart, M.B. Rook, M.A.G. van, der Heyden, L.H. Heitman, A.P. IJzerman, Structure–affinity relationships (SARs) and structure–kinetics relationships (SKRs) of Kv11.1 blockers, J. Med. Chem. 58 (15) (2015) 5916–5929.

[42] Z. Yu, A.P. IJzerman, L.H. Heitman, K(v)11.1 (hERG)-induced cardiotoxicity: a molecular insight from a binding kinetics study of prototypical K(v)11.1 (hERG) inhibitors, Br. J. Pharmacol. 172 (3) (2015) 940–955.

[43] G.F. Smith, Medicinal chemistry by the numbers: the physicochemistry, thermodynamics and kinetics of modern drug design, in: G. Lawton, D.R. Witty (Eds.), Progress in Medicinal Chemistry, Elsevier B.V, Burlington, 2009, p. 1.

[44] C. Gallo-Rodriguez, X.-D. Ji, N. Melman, B.D. Siegman, L.H. Sanders, J. Orlina, B. Fischer, Q. Pu, M.E. Olah, P.J.M. van Galen, G.L. Stiles, K.A. Jacobson, Structure–activity relationships of N^6-benzyladenosine-5′-uronamides as A_3-selective adenosine agonists, J. Med. Chem. 37 (5) (1994) 636–646.

[45] D. Guo, L.H. Heitman, A.P. IJzerman, Kinetic aspects of the interaction between ligand and G protein-coupled receptor: the case of the adenosine receptors, Chem. Rev. 117 (1) (2017) 38–66.

[46] K.-N. Klotz, N. Falgner, S. Kachler, C. Lambertucci, S. Vittori, R. Volpini, G. Cristalli, [^{3}H]HEMADO— a novel tritiated agonist selective for the human adenosine A_3 receptor, Eur. J. Pharmacol. 556 (1) (2007) 14–18.

[47] J.A. Auchampach, E.T. Gizewski, T.C. Wan, S. de Castro, G.G. Brown, K.A. Jacobson, Synthesis and pharmacological characterization of [^{125}I]MRS5127, a high affinity, selective agonist radioligand for the A_3 adenosine receptor, Biochem. Pharmacol. 79 (7) (2010) 967–973.

[48] D. Guo, L. Xia, J.P.D. van Veldhoven, M. Hazeu, T. Mocking, J. Brussee, A.P. IJzerman, L.H. Heitman, Binding kinetics of ZM241385 derivatives at the human adenosine A_{2A} receptor, ChemMedChem 9 (4) (2014) 752–761.

[49] A. Glukhova, D.M. Thal, A.T. Nguyen, E.A. Vecchio, M. Jörg, P.J. Scammells, L.T. May, P.M. Sexton, A. Christopoulos, Structure of the adenosine A_1 receptor reveals the basis for subtype selectivity, Cell 168 (5) (2017) 867–877.

[50] A. Ciancetta, K. Jacobson, Structural probing and molecular modeling of the A_3 adenosine receptor: a focus on agonist binding, Molecules 22 (3) (2017) 449–466.

[51] D. Guo, A.C. Pan, R.O. Dror, T. Mocking, R. Liu, L.H. Heitman, D.E. Shaw, A.P. IJzerman, Molecular basis of ligand dissociation from the adenosine A_{2A} receptor, Mol. Pharmacol. 89 (5) (2016) 485–491.

[52] W. Liu, E. Chun, A.A. Thompson, P. Chubukov, F. Xu, V. Katritch, G.W. Han, C.B. Roth, L.H. Heitman, A.P. IJzerman, V. Cherezov, R.C. Stevens, Structural basis for allosteric regulation of GPCRs by sodium ions, Science 337 (6091) (2012) 232–236.

[53] E. Segala, D. Guo, R.K.Y. Cheng, A. Bortolato, F. Deflorian, A.S. Doré, J.C. Errey, L. H. Heitman, A.P. IJzerman, F.H. Marshall, R.M. Cooke, Controlling the dissociation of ligands from the adenosine A_{2A} receptor through modulation of salt bridge strength, J. Med. Chem. 59 (13) (2016) 6470–6479.

[54] Z. Xu, Y. Jang, R.A. Mueller, E.A. Norfleet, IB-MECA and cardioprotection, Cardiovasc. Drug Rev. 24 (3–4) (2006) 227–238.

[55] Z.-D. Ge, J.N. Peart, L.M. Kreckler, T.C. Wan, M.A. Jacobson, G.J. Gross, J.A. Auchampach, Cl-IB-MECA [2-chloro-N^6-(3-iodobenzyl)adenosine-5′-N-methylcarboxamide] reduces ischemia/reperfusion injury in mice by activating the A_3 adenosine receptor, J. Pharmacol. Exp. Ther. 319 (3) (2006) 1200–1210.

[56] National center for biotechnology information. Pubchem compound database; CID=123683, https://pubchem.ncbi.nlm.nih.gov/compound/123683 (accessed June 30, 2017).

[57] National center for biotechnology information. PubChem compound database; CID=3035850, https://pubchem.ncbi.nlm.nih.gov/compound/3035850 (accessed June 30, 2017).

[58] Z. Chen, K. Janes, C. Chen, T. Doyle, L. Bryant, D.K. Tosh, K.A. Jacobson, D. Salvemini, Controlling murine and rat chronic pain through A_3 adenosine receptor activation, FASEB J. 26 (5) (2012) 1855–1865.

[59] J.L. Carlin, D.K. Tosh, C. Xiao, R.A. Piñol, Z. Chen, D. Salvemini, O. Gavrilova, K.A. Jacobson, M.L. Reitman, Peripheral adenosine A_3 receptor activation causes regulated hypothermia in mice that is dependent on central histamine H_1 receptors, J. Pharmacol. Exp. Ther. 356 (2) (2016) 474–482.

[60] J.W. Little, A. Ford, A.M. Symons-Liguori, Z. Chen, K. Janes, T. Doyle, J. Xie, L. Luongo, D.K. Tosh, S. Maione, K. Bannister, A.H. Dickenson, T.W. Vanderah, F. Porreca, K.A. Jacobson, D. Salvemini, Endogenous adenosine A_3 receptor activation selectively alleviates persistent pain states, Brain 138 (1) (2015) 28–35.

[61] A. Ford, A. Castonguay, M. Cottet, J.W. Little, Z. Chen, A.M. Symons-Liguori, T. Doyle, T.M. Egan, T.W. Vanderah, Y. De Konnick, D.K. Tosh, K.A. Jacobson, D. Salvemini, Engagement of the GABA to KCC2 signaling pathway contributes to the analgesic effects of A_3AR agonists in neuropathic pain, J. Neurosci. 35 (15) (2015) 6057–6067.

[62] W.E.A. de Witte, M. Danhof, P.H. van der Graaf, E.C.M. de Lange, In vivo target residence time and kinetic selectivity: the association rate constant as determinant, Trends Pharmacol. Sci. 37 (10) (2016) 831–842.